ORIGINAL ARTICLE

WILEY

Inactivation of aerosolized SARS-CoV-2 by 254 nm UV-C irradiation

Natalia Ruetalo[1] | Simon Berger[2] | Jennifer Niessner[2] | Michael Schindler[1]

[1]Institute for Medical Virology and Epidemiology of Viral Diseases, University Hospital Tübingen, Tübingen, Germany

[2]Institute for Flow in Additively Manufactured Porous Media, Hochschule Heilbronn, Heilbronn, Germany

Correspondence
Michael Schindler, Institute for Medical Virology and Epidemiology of Viral Diseases, University Hospital Tübingen, Tübingen, Germany.
Email: michael.schindler@med.uni-tuebingen.de

Jennifer Niessner, Institute for Flow in Additively Manufactured Porous Media, Hochschule Heilbronn, Heilbronn, Germany.
Email: jennifer.niessner@hs-heilbronn.de

Abstract

Surface residing SARS-CoV-2 is efficiently inactivated by UV-C irradiation. This raises the question whether UV-C-based technologies are also suitable to decontaminate SARS-CoV-2- containing aerosols and which doses are needed to achieve inactivation. Here, we designed a test bench to generate aerosolized SARS-CoV-2 and exposed the aerosols to a defined UV-C dose. Our results demonstrate that the exposure of aerosolized SARS-CoV-2 with a low average dose in the order of 0.42–0.51 mJ/cm^2 UV-C at 254 nm resulted in more than 99.9% reduction in viral titers. Altogether, UV-C-based decontamination of aerosols seems highly effective to achieve a significant reduction in SARS-CoV-2 infectivity.

KEYWORDS
aerosol, Covid-19, decontamination, inactivation, SARS-CoV-2, UV-C

1 | INTRODUCTION

Severe acute respiratory syndrome coronavirus-2 (SARS-CoV-2), the causative agent of COVID-19, has spread since January 2020, leading to global health and social crisis. Although early on, the consensus pointed to direct contact and large droplets as the main source of infection, there is now growing evidence that the virus is transmitted by aerosols,[1] which might be even the main route of transmission.[2] Aerosols, as the major transmission route, better explains the superspreading events and the large proportion of infections generated from asymptomatic people.[3] Small aerosol particles can be suspended and travel through the air. In the case of SARS-CoV-2, it was shown that they can remain viable for 3 h and float for several hours.[4] In this context, there is an urgent need for technologies that allow decontamination of breathing air, for instance, in public transportation, schools, hospitals, and many other settings. Currently, mechanical (mainly HEPA14 and 13) filters are used for such purposes with certain limitations related to the size, energy demand, noise, capacity, and need for ongoing maintenance. Other inactivating technologies, based for instance on cold plasma and ultraviolet germicidal irradiation using UV-C are discussed and partly already in use.

UV-C disinfection has been used for several decades to inactivate different infectious agents, including fungi, bacteria, and viruses, both from contaminated liquids and surfaces.[5-7] Although the primary mode of action for UV inactivation is considered to be genome damaging through the formation of pyrimidine dimers[8-10] different mechanisms have been described. These include protein oxidation, destruction of the capsid protein, and crosslinking of viral genome-protein.[11] Regarding decontamination of coronaviruses, it was previously shown that non-human coronaviruses as well as common-cold coronaviruses and SARS-CoV are sensitive to

---

Natalia Ruetalo and Simon Berger contributed equally and are co-first authors.

inactivation by UV-C irradiation.[10,12–16] Accordingly, as expected, our group and others have demonstrated that SARS-CoV-2 can also be UV-inactivated from liquids and dried surfaces.[17–27] Although some studies published high UV-C doses of 100–300 mJ/cm² to be required for reaching 1-log reduction on viral titers,[16,22] the vast majority of studies performed at 254 nm irradiation, reported doses ranging from 1.2 to 7 mJ/cm² to achieve the same reduction. Regarding wavelengths, studies focused on coronaviruses reported similar required doses compared with 254 nm when UV-LED 222 nm irradiation was used[15,21] and approximately two times higher doses by applying UV-C at 280 nm wavelength.[15,20] Within the same experimental approach, Ma et al.[15] showed a dependency of the required dose according to the wavelength used for irradiation.

For inactivation of virus-containing aerosols in general[28–30] and coronaviruses in particular, literature is sparse and there is virtually no information on minimal UV-C doses necessary to inactivate SARS-CoV-2.[31] In this context, we designed, built, and established a test bench to evaluate UV-C mediated SARS-CoV-2 inactivation in aerosols and determine the potency of a low dose of 254 nm UV-C irradiation to reduce viral titers.

2 | MATERIALS AND METHODS

2.1 | Design and building of the test bench

We designed and built a test bench allowing for the nebulization of suspended SARS-CoV-2 and the exposure of the generated virus-containing aerosol particles by different doses of UV-C irradiation in a laminar flow cabinet of a BSL3 lab. Detailed information on the experimental set-up and the calculation of UV-C doses is given in the Data S1 and the Figures S1–S5.

As schematically shown in Figure 1, essential components of the testing rig are an aerosol generator, an UV-C lamp, and a test section.

2.2 | Aerosol generator

For aerosol generation, the "Portable Aerosol Generator" (PAG) 1000 (Palas GmbH) was used. The PAG 1000 uses a Laskin nozzle that is completely immersed in test suspension. With this principle, compressed air is led through small air jet holes in the Laskin nozzle and is thus strongly accelerated. As a result, the test suspension flows into a collar ring located above the jet holes. Subsequently, the pressurized air entrains and disperses particles of the liquid inflow sidelong the collar ring, which leads to the formation of particle containing gas bubbles. As these bubbles rise in the test suspension and reach the liquid surface, the particles are aerosolized.

2.3 | UV-C lamp

Inactivation experiments were conducted using monochromatic UV-C irradiation at a wavelength of 254 nm. Therefore, a

Practical Implications

- Generation of contagious SARS-CoV-2 containing aerosols under BSL3 conditions.
- Design of a test bench to expose virus-laden aerosols to defined doses of UV-C, thereby allowing to assess virus inactivation in aerosols.
- A UV-C dose at 254 nm in the order of 0.42–0.51 mJ/cm² reduces more than 99.9% of SARS-CoV-2 infectivity in aerosols.
- This helps to design rational based disinfection devices that inactivate SARS-CoV-2 in aerosols by 254 nm UV-C irradiation.

low-pressure mercury vapor discharge lamp (NNI 201/107 XL, Heraeus Noblelight GmbH) was used and mounted outside the test section.

2.4 | Test section

Aerosols are injected at the beginning of the test section perpendicular to UV-C impermeable vacuum tube components and diluted with ambient air from inside the laminar flow cabinet. Here, a mass flow controller (Vögtlin GmbH) and a vacuum pump (Pfeiffer Vacuum GmbH) ensure a constant total volume flow. Next, the diluted aerosol is exposed to UV-C irradiation in an UV-C transmissive and 50 cm long fused silica tube section (Heraeus Noblelight GmbH). The UV-C irradiance, on the one hand, is directly influenced by the lamp distance to the fused silica tube and therefore can be set via a moveable carriage on which the lamp is mounted. The exposure time, on the other hand, is dependent on flow velocity, and thus can be varied using fused silica tubes in three different diameters (11, 17 and 30 mm) and adjustable total volume flows (5–20 L/min). As a result, UV-C doses from 0.36 to 28 mJ/cm² can be achieved (see Figure S5). To sample aerosol particles thereafter, the aerosol passes a flat sheet holder, which is equipped with gelatine filter membranes (Sartorius AG). As humidity, temperature, and ozone can in principle affect infectivity, these quantities are determined downstream the sampling point to exclude inactivating side effects additional to UV-C inactivation. In our setup, we did not detect elevated levels of ozone in the system. At the end of the test section, the air is purified using a HEPA H14 filter (ELSÄSSER Filtertechnik GmbH) and released via the mass flow controller in series with a vacuum pump into the laminar flow.

2.5 | Cell culture

Caco-2 (human colorectal adenocarcinoma) cells were cultured at 37°C with 5% CO₂ in Dulbecco modified Eagle medium containing 10% fetal calf serum (FCS), with 2 mM L-glutamine, 100 mg/ml penicillin–streptomycin, and 1% nonessential amino acids.

FIGURE 1 Schematic representation of the testing rig (upper graph) and picture of the experimental setup in the laminar flow cabinet of the BSL3 laboratory (lower picture)
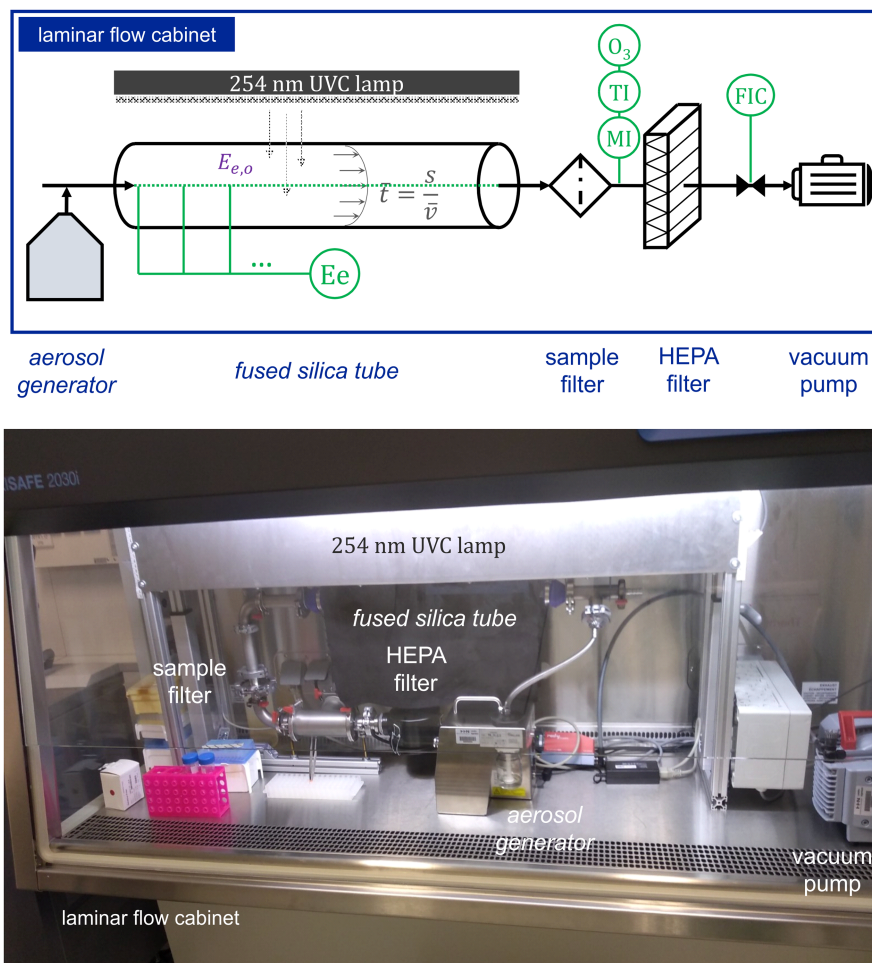
2.6 | Virus isolate

The recombinant SARS-CoV-2 expressing mNeonGreen (icSARS-CoV-2-mNG)[32] was obtained from the World Reference Center for Emerging Viruses and Arboviruses (WRCEVA) at the UTMB (University of Texas Medical Branch). The generation of SARS-CoV-2-mNG stocks as well as the determination of viral titers and multiplicity of infection was described previously.[33] To eliminate the cell culture media, the viral stock was purified using 20% sucrose centrifugation ($20000\,g$, 90 min, 4°C). After a PBS-wash step, the pellet was resuspended in PBS using the same volume as the original viral stock.

2.7 | Aerosol generation

For aerosol generation, 1–3 ml of viral stock was purified and re-suspended in 1 ml PBS and further diluted to 30 ml total volume with PBS (dead volume of the PAG 1000). Titers were determined for each experiment using the titration of the "stock" as an internal control. The PAG was operated at room temperature, at maximum settings and the total flow rate was set to 20 L/min. Aerosols were produced in a range from 1 to 10 min. After generation, aerosol particles were recovered from gelatin filters (2602-037-ALK, Sartorius).

Filters were dissolved in 1 ml infection media (cell culture media with 5% FCS) for 10 min at 37°C. This media containing the recovered infectivity was titrated in 2-fold serial dilutions on Caco-2 cells. According to the specifications of the manufacturer, the PAG 1000 can aerosolize a maximum of 0.9 g/h (Diethyl-Hexyl-Sebacat particles). Using this parameter, we estimated roughly that the maximum aerosolized volume could be 0.015 ml/min. Therefore, as internal reference, 75 µl (theoretical volume aerosolized in 5 min) of the diluted stock (1:30–1:10 according to each experiment) were diluted either in 1 ml of infection media ("stock") or in 1 ml of infection media where a gelatin filter was previously dissolved ("stock + filter").

2.8 | UV-C inactivation of aerosols

Aerosol particles were generated using the PAG 1000. Therefore, 6 ml of viral stock was purified, re-suspended in PBS, and diluted to a total volume of 60 ml with PBS. The diluted stock was divided into two aliquots (30 ml each), one used to produce aerosol particles for 2 min using the conditions already described, and the other one to repeat this experiment under UV-C exposure. The UV-C lamp was on for 400 s before starting aerosol generation in order to reach a constant UV-C intensity according to the manufacturers' specification. For these first experiments, we used a low UV-C dose. It was

applied using a distance of 25 cm, tube diameter of 11 mm, and a flow of 20 l/min. Neglecting transmission losses of the fused silica tube this corresponds to the maximum mean radiant exposure of 0.51 mJ/cm^2. If transmission losses are considered according to the measurement described in the Data S1 a total average dose of 0.42 mJ/cm^2 can be assumed (Figure S5).

2.9 | Evaluation of recovered infectivity

1×10^4 Caco-2 cells/well were seeded in 96-well plates the day before infection. After aerosol generation, cells were infected in 2-fold serial dilutions using the media-containing filter-recovered aerosol particles or mock-infected. Forty-eight hours post-infection (hpi) cells were fixed with 2% PFA and counter-stained with Hoechst 33342 (1 μg/ml final concentration) for 10 min at 37°C. The staining solution was removed and exchanged for PBS. Using an imaging plate reader (Cytation3, BioTek), images of all wells were taken in the green channel to detect the infected fluorescent (mNG) cells and in the blue channel for the cellular nucleus, stained with Hoechst. All infected cells (mNG+) and the total number of cells in each well (Hoechst+) were counted with the automatic Gen5 software of the plate reader. The infection rate was then calculated as N° of mNG+/ N° of Hoechst+.

2.10 | Statistical analysis

All calculations regarding mean values, SEM and other statistical tests were done using GraphPad Prism 9.

3 | RESULTS

3.1 | Virus stock preparation and recovery of infectious SARS-CoV-2 via gelatin filters

The aerosol test device (Figure 1) was installed under a sterile bench, such as that highly infectious aerosol-borne pathogens can be analyzed inside a BSL3 lab. Initial experiments with SARS-CoV-2 viral stocks produced in standard cell culture media revealed extensive foam formation, precluding standardized and safe aerosol generation. We hence decided to purify SARS-CoV-2 viral stocks via sucrose and resuspend the purified virus in PBS, to avoid foam formation by the aerosolization process. We further upscaled the volume to 30 ml, as this is the minimum volume to be used in the PAG 1000 for aerosol generation. Importantly, purification and resuspension of virus stock in PBS does not result in reduced infectivity (Figure 2), allowing foam-free aerosol generation.

To recover SARS-CoV-2 aerosolized particles, we employed gelatin filters that can be solubilized in media at 37°C. Therefore, we tested whether the chemical composition of the filter might reduce infectivity and virus stability. For this purpose, we diluted the virus

stock 1:30 into 1 ml of infection media, 1 ml of PBS, or 1 ml of PBS in which a filter was dissolved. The three preparations were then used to infect Caco-2 cells and assess viral titers (Figure 3). Diluting the virus in presence of the gelatin filters does not result in a loss of viral infectivity. In addition, cell viability is also not affected by any filter component.

3.2 | Generation and recovery of SARS-CoV-2 containing aerosols

Next, we analyzed aerosol generation by the PAG 1000 and recovery via gelatin filters in our test bench. To increase the amount of aerosolized virus, we increased virus concentration threefold as compared with the previous experiments by purifying 3 ml of virus stock that was resuspended in 30 ml of PBS. As controls, we took 75 μl of diluted virus stock (see Section 2) and diluted the preparations in 1 ml of media ("stock") or in 1 ml of media in which a gelatin filter was previously dissolved ("filter + stock"). Initially, we evaluated different aerosol generation times, including 5 and 10 min (Figure 4). Using this system, we were able to generate aerosolized SARS-CoV-2 viral particles, which after recovery, were still capable of infecting cells. Paradoxically, while the infectivity recovered after 5 min of aerosol generation showed similar titers as the "stock" control, we did not recover any, or the recovery was substantially lower, after additional 10 min of aerosol generation. From this data, we hypothesized that aerosol generation per se, using this system leads to a loss of viral infectivity.

To evaluate the hypothesis of a potential inactivation of SARS-CoV-2 in the flask (Schott bottle) used for aerosolization with the PAG 1000, we measured the infectivity of the virus stock directly in the flask after different time points of aerosol generation. This revealed that the infectivity of the virus in aliquots taken directly from the bottle after 10 min of aerosol generation was reduced, and after 20 min, we detected barely any infectious virus (Figure 5). Hence, the process of aerosols generation by the PAG 1000 itself leads to a loss of SARS-CoV-2 infectivity, most likely due to the generated shear forces during multiple passes of test suspension through the Laskin nozzle.

3.3 | Aerosol-containing SARS-CoV-2 is efficiently inactivated by 254 nm UV-C irradiation

The aerosolization process itself does not affect SARS-CoV-2 infectivity at 2 and 5 min of aerosol generation (Figure 5) and we were able to recover SARS-CoV-2 containing aerosols from filters after 5 min of aerosol generation (Figure 4). We therefore decided to initiate UV-C inactivation experiments of SARS-CoV-2 containing aerosols using 2 min of aerosol generation, as an intermediate timepoint between good yields of infectivity and low probability of harmful effects of the aerosolization process. To avoid the intrinsic inactivation effect, we generated enough virus to exchange the stock in the
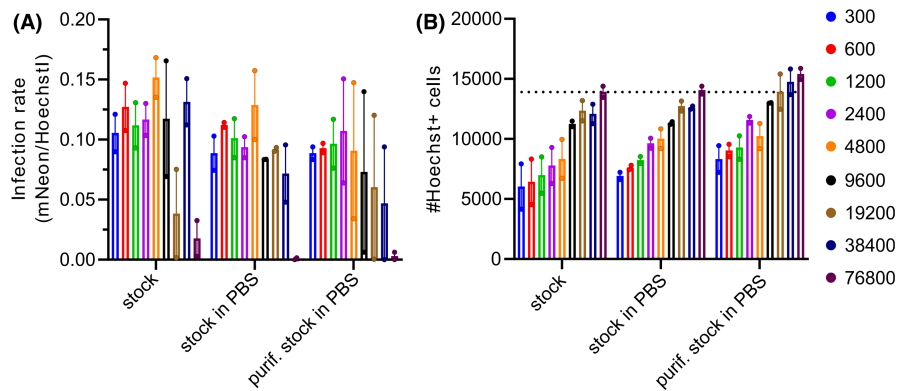
FIGURE 2 SARS-CoV-2 infectivity after virus purification and resuspension in PBS. SARS-CoV-2-mNG stock was produced under standard conditions, diluted in PBS, or sucrose purified and resuspended in PBS as described in the Section 2. Thereafter, Caco-2 cells were infected with serial dilutions of the different virus stock preparations. 48 h post-infection (hpi) cells were fixed, stained with Hoechst, and measured with the Cytation3 imaging systems. The left graph (A) indicates the individual infection rate based on the virus-genome expressed quantification of mNG related to the total amount of cells (mNG+/Hoechst+ cells). The right graph (B) shows the absolute number of cells per well (#Hoechst+ cells). Mean and standard deviation (SEM) shown is from duplicate infections.
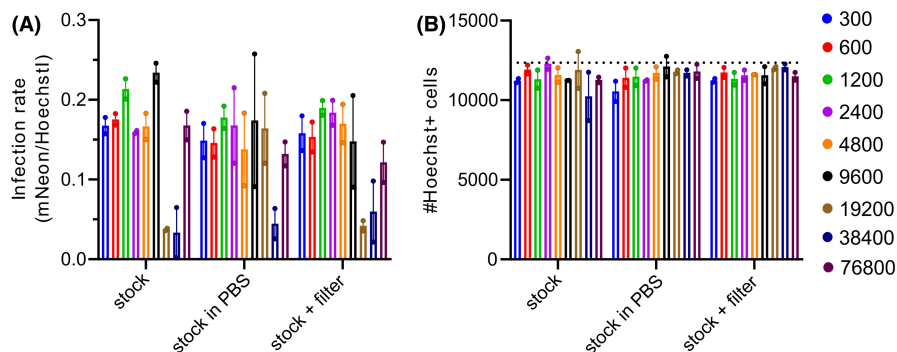

FIGURE 3 SARS-CoV-2 infectivity is not affected by the gelatin filter. SARS-CoV-2-mNG stock was produced under standard conditions. Virus stock was diluted in 1 ml infection media, PBS, or PBS in which a gelatin filter was dissolved. Caco-2 cells were infected with serial dilutions of the different preparations. 48 hpi cells were fixed, stained with Hoechst, and measured with the Cytation3 imaging systems. Left graph (A) indicates the individual infection rate based on the virus-genome expressed quantification of mNG related to the total amount of cells (mNG+/Hoechst+ cells). The right graph (B) shows the absolute number of cells per well (#Hoechst+ cells). Mean and standard deviation (SEM) shown is from duplicate infections.

bottle after each experimental run. Figure 6 shows the result of an experiment in which we first aerosolized SARS-CoV-2 for 2 min, isolated the infectivity from the gelatin filter, exchanged the virus stock in the bottle, and repeated the same experiment with the UV-C lamp turned on at a distance of 25 cm to the glass tube. The setting, corresponds to a total dose of 0.42 mJ/cm^2 at 254 nm UV-C irradiation when transmission losses due to the fused silica are considered (Figure S5), but a highest possible dose of 0.51 mJ/cm^2 when these losses are neglected. Of note, this procedure leads to a strong reduction of SARS-CoV-2 infectivity (Figure 6).

From the serial dilutions, we calculated the input titer of the virus stock recovered from the filter (2.9 × 10^6 IU/ml) versus the titer in the aerosol after 0.42–0.51 mJ/cm^2 UV-C exposure (10.834 IU/ml). From this, we calculated a titer reduction >99.9%. Hence, a conservative interpretation of our results allows the conclusion that a relatively low average dose in the order of 0.42–0.51 mJ/cm^2 at 254 nm allows for more than two-log reduction in aerosolized SARS-CoV-2 infectivity.

4 | DISCUSSION

Decontamination of wastewater or surfaces by UV-C irradiation is an established and highly effective technique to inactivate bacteria or viruses.[7,34] Doses necessary for pathogen inactivation vary substantially dependent on specific pathogen characteristics. UV-C doses required to inactivate fungal spores, fungal cells, and yeast (~250 mJ/cm^2) as well as bacterial spores (~150 mJ/cm^2), are typically higher compared with bacteria and viruses (30–40 mJ/cm^2) (1-log reduction in water), although values can vary drastically within each group.[9] Regarding viruses, non-enveloped viruses need higher UV-C doses since their protein shell is more stable as compared with enveloped viruses, and viruses with an RNA genome are easier to inactivate than viruses with a DNA genome, due to the fact the RNA is more labile than DNA.[10,35] Furthermore, the same pathogen might need different doses of UV-C for inactivation when it is dried on surfaces, present in wastewater, or in aerosols.[9] In addition, the use of different wavelengths also influences the required UV dose,[15] most likely
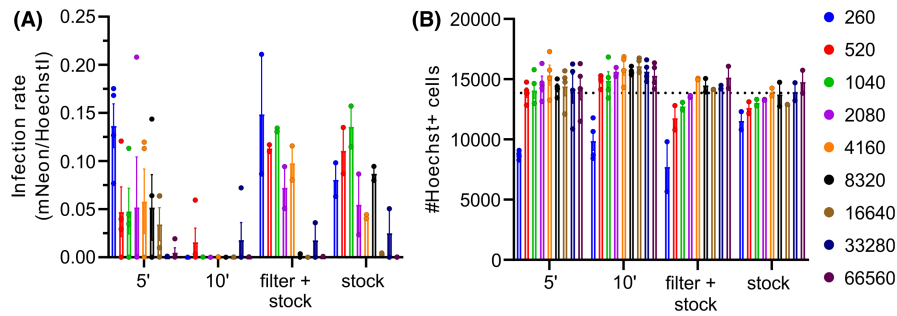
FIGURE 4 SARS-CoV-2 infectivity recovered from aerosols. SARS-CoV-2-mNG stock was produced under standard conditions, purified, resuspended in PBS, and diluted 1:10 in PBS. Aerosols were generated for 5 or 10 min with the PAG 1000 directly connected to the recovery filter. Gelatin filters used for virus recovery were dissolved in 1 ml infection media. Furthermore, 75 μl of virus stock were diluted in 1 ml infection media in which a filter was dissolved (filter + stock), or 75 μl were directly diluted in 1 ml infection media (stock). Caco-2 cells were infected with serial dilutions of the different preparations. 48 hpi cells were fixed, stained with Hoechst. and measured with the Cytation3 imaging systems. Left graph (A) indicates the individual infection rate based on the virus-genome expressed quantification of mNG related to the total amount of cells (mNG+/Hoechst+ cells). The right graph (B) shows the absolute number of cells per well (#Hoechst+ cells). Mean and standard deviation (SEM) shown is from two experiments with duplicate infections.
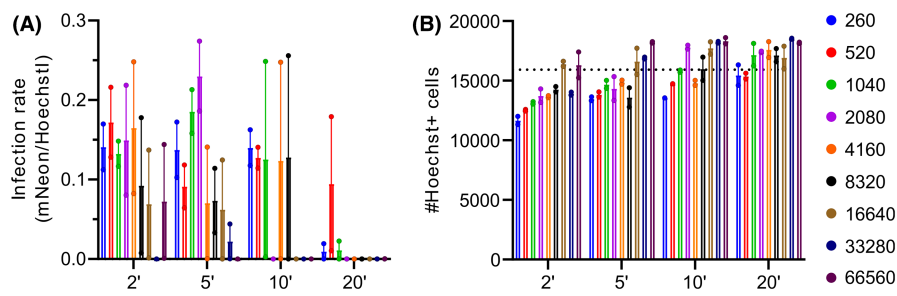

FIGURE 5 Aerosolization process itself affects SARS-CoV-2 infectivity. SARS-CoV-2-mNG stock was produced under standard conditions, purified, resuspended in PBS, and diluted 1:10 in PBS. 75 μl aliquots were directly taken from the Schott bottle plugged into the PAG 1000 after 2, 5, 10, and 20 min of aerosol generation. Each aliquot was diluted in 1 ml infection media and Caco-2 cells were infected with serial dilutions of the different preparations. 48 hpi cells were fixed, stained with Hoechst, and measured with the Cytation3 imaging systems. Left graph (A) indicates the individual infection rate based on the virus-genome expressed quantification of mNG related to the total amount of cells (mNG+/Hoechst+ cells). The right graph (B) shows the absolute number of cells per well (#Hoechst+ cells). Mean and standard deviation (SEM) shown is from duplicate infections.

by altering the inactivation mechanism. Recently, Oh et al.[36] showed that the UV inactivation of Adenovirus, one of the most UV-resistant viruses, was more efficiently inactivated at 222 nm than at 254 nm. Besides, the inactivation at 222 nm depended mostly on the damage of the capsid protein, claiming that UV at 222 nm primarily targets AdV capsid proteins, while monochromatic UV at 254 nm mostly attacks the genome.

Several groups, including our laboratory[17–27] evaluated the sensitivity of SARS-CoV-2 towards UV-C irradiation, mainly using surface-dried viruses or liquid viral stocks. While it is clear that SARS-CoV-2 is inactivated by UV-C, doses reported vary substantially. Many parameters can be the reason for this variation, including initial titers of the stock used, optical absorbance of the sample to be irradiated, environmental conditions (humidity, textured surfaces) experimental setup for UV exposure (distance, placement of the sample respect to the source, lamp features), read-out of the experiment and calculation for UV doses.[19,26,27] In this context, we

reported >6-log reduction of surface dried SARS-CoV-2 by a UV-C dose of 3.5 mJ/cm^2 and a non-linear decay in the inactivation efficiency as 1.75 mJ/cm^2 reduced viral titers only by 1-log in the same setting.[17] This value is roughly in the same range as the majority of the mentioned studies, reporting 1.2–7 mJ/cm^2 for 1-log reduction. In addition, what should be also considered for comparing results among studies is the non-linear decay observation we reported previously[17] which can be also confirmed by analyzing other studies.[24] Although highly relevant, UV-C mediated decontamination of aerosolized viruses, in particular SARS-CoV-2, is an understudied topic. We are aware of only four publications[28–31] trying to assess the stability of coronaviruses in aerosols. Walker et al.,[28] demonstrated that murine beta coronaviruses aerosols are highly susceptible to 254 nm UV-C-irradiation, between 7 and 10 times more than adenoviruses and bacteriophage MS2. Another study[7] employed a setup similar to ours, however, in dimensions precluding applications in a standard BSL-3, as the device had a
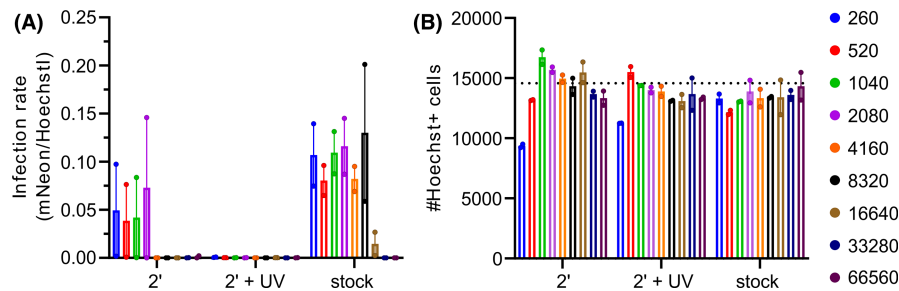
FIGURE 6 SARS-CoV-2 aerosols are inactivated by 254 nm UV-C irradiation. SARS-CoV-2-mNG stock was produced under standard conditions, purified, resuspended in PBS, and diluted 1:10 in PBS. Aerosols were generated for 2 min with the PAG 1000 in the test bench shown in Figure 1. After generation, the gelatin filter was removed and dissolved in 1 ml infection media. The experiment was repeated with the 254 nm UV-C lamp turned on (total average UV-C dose of $0.42\,mJ/cm^2$, maximum total average dose of $0.51\,mJ/cm^2$ neglecting transmission losses). As control, 75 μl of virus stock were directly dissolved in 1 ml infection media (the back-calculated titer of the stock was $5.6 \times 10^6\,IU/ml$). Caco-2 cells were infected with serial dilutions of the preparations. 48 hpi cells were fixed, stained with Hoechst, and measured with the Cytation3 imaging systems. The left graph (A) indicates the individual infection rate based on the virus-genome expressed quantification of mNG related to the total amount of cells (mNG+/Hoechst+ cells). The right graph (B) shows the absolute number of cells per well (#Hoechst+ cells). Mean and standard deviation (SEM) shown is from duplicate infections. Similar results were obtained in one additional experiment.

total dimension of several meters and was placed in a 3.8 m wind tunnel. The authors used porcine respiratory coronavirus and as they had fixed UV-C lamps they found a dose of 13.9 mJ/cm² achieving >2.2-log reduction in viral titers.[30] Buonanno et al.[29] investigated the inactivation of aerosolized common cold coronaviruses and influenza, determining low doses ranging from 1.2 to 3.8 mJ/cm² to achieve 3-log reduction, using far-UV-C light at 222 nm. Finally, only one study worked with SARS-CoV-2 using a commercial system employing UV-C or ozone to inactivate this virus and the seasonal HCoV-OC43.[31] Their experimental setup did not facilitate the determination of irradiation doses or recovery of infectious viruses. They reported that after 120 and 90 min of irradiation for HCoV-OC43 and SARS-CoV-2, respectively, viral RNA was no longer detected by qRT-PCR. However, whether the viruses lose infectivity before or remain infectious even after treatment was not evaluated. In our system, an average dose in the order of 0.42–0.51 mJ/cm² inactivated more than 99.9% of infectious particles indicating that aerosol-borne SARS-CoV-2 is more efficiently inactivated than a surface dried virus, which possibly complexes with serum proteins and other molecules present in culture media. This difference might be influenced by the fact that the virus was dried in the presence of media, while the aerosol-inactivated virus was previously purified and resuspended in PBS. Even though speculative, it was already observed that viruses in general are easier to inactivate in air than in water or on dried surfaces,[9] where the organic components present in the media can exert a shielding effect.[26]

While our experiments give a first promising indication for the UV-C sensitivity of SARS-CoV-2 in aerosols, there are a variety of open questions and experiments to be done. First of all, we have to perform additional independent experiments with different UV-C doses to establish a firm dose–response curve. Furthermore, we have used a mNeonGreen expressing reporter virus based on one of the first Wuhan SARS-CoV-2 isolates. Even though it is unlikely since UV-C mediated inactivation of SARS-CoV-2 is largely based on damaging the viral genome,[11] the infectivity and stability of currently circulating SARS-CoV-2 variants might differ. Indeed, Inagaki et al.[37] showed a difference in the 280 nm UV dose required to inactive alpha, beta, and gamma SARS-CoV-2 variants of concern. It will be important to confirm this result and compare doses necessary for inactivation of the Delta and Omicron isolates. In addition, different UV-C irradiation sources are available in terms of wavelength, which will differ in the UV-C doses and should be evaluated (for instance LED-based UV-C sources or Far UV-C excimer lamps).

The major obstacle to reliable data related to the UV-C mediated inactivation of SARS-CoV-2 is associated with severe difficulties to generate and recover aerosols of this highly contagious and pathogenic virus in a standardized manner under BSL-3 conditions. Furthermore, it is necessary to carefully expose these aerosols to defined doses of UV-C irradiation. With the test bench designed and presented here, we have overcome these problems and offer a solution to evaluate the dose–response relationship between UV-C exposure and decontamination of SARS-CoV-2 containing aerosols.

AUTHOR CONTRIBUTIONS

NR, SB, JN, and MS conceived and designed the study. NR and MS planned the virus inactivation experiments. SB and JN planned the design of the test bench. SB built the test bench. SB and JN performed measurement rows with the test bench to analyze aerosol generation parameters. NR conducted the virus inactivation experiments and all experiments with aerosolized SARS-CoV-2. NR and MS analyzed the virus inactivation data. NR, SB, JN, and MS wrote the initial manuscript draft. NR and MS developed the manuscript to its final form. NR, SB, JN, and MS did proofreading and editing of the final manuscript.

ACKNOWLEDGMENTS

CONFLICT OF INTEREST

The authors have no conflict of interest to declare.

DATA AVAILABILITY STATEMENT

All data are included in the manuscript and its supplemental files.

ORCID

Michael Schindler https://orcid.org/0000-0001-8989-5813

REFERENCES

1. Karmacharya M, Kumar S, Gulenko O, Cho YK. Advances in facemasks during the COVID-19 pandemic era. *ACS Appl Bio Mater.* 2021;4:3891-3908.
2. Nardell EA. Air disinfection for airborne infection control with a focus on COVID-19: why germicidal UV is essential. *Photochem Photobiol.* 2021;97:493-497.
3. Viana Martins CP, Xavier CSF, Cobrado L. Disinfection methods against SARS-CoV-2: a systematic review. *J Hosp Infect.* 2022;119:84-117.
4. van Doremalen N, Bushmaker T, Morris DH, et al. Aerosol and surface stability of SARS-CoV-2 as compared with SARS-CoV-1. *N Engl J Med.* 2020;382:1564-1567.
5. Qureshi Z, Yassin MH. Role of ultraviolet (UV) disinfection in infection control and environmental cleaning. *Infect Disord Drug Targets.* 2013;13:191-195.
6. Kowalski WJ, Bahnfleth WP, Raguse M, Moeller R. The cluster model of ultraviolet disinfection explains tailing kinetics. *J Appl Microbiol.* 2020;128:1003-1014.
7. Malayeri AD, Mohseni M, Cairns B, et al. Fluence (UV dose) required to achieve incremental log inactivation of Bacteria, Protozoa, Viruses and Algae. *IUVA News.* 2016;18:4–6.
8. Hessling M, Hones K, Vatter P, Lingenfelder C. Ultraviolet irradiation doses for coronavirus inactivation – review and analysis of coronavirus photoinactivation studies. *GMS Hyg Infect Control.* 2020;15:Doc08.
9. Kowalski W. *Ultraviolet Germicidal Irradiation Handbook: UVGI for Air and Surface Disinfection.* Springer, Heidelberg; 2009.
10. Tseng CC, Li CS. Inactivation of viruses on surfaces by ultraviolet germicidal irradiation. *J Occup Environ Hyg.* 2007;4:400-405.
11. Lo CW, Matsuura R, Iimura K, et al. UVC disinfects SARS-CoV-2 by induction of viral genome damage without apparent effects on viral morphology and proteins. *Sci Rep.* 2021;11:13804.
12. Duan SM, Zhao XS, Wen RF, et al. Stability of SARS coronavirus in human specimens and environment and its sensitivity to heating and UV irradiation. *Biomed Environ Sci.* 2003;16:246-255.
13. Tsunetsugu-Yokota Y. Large-scale preparation of UV-inactivated SARS coronavirus virions for vaccine antigen. *Methods Mol Biol.* 2008;454:119-126.
14. Kariwa H, Fujii N, Takashima I. Inactivation of SARS coronavirus by means of povidone-iodine, physical conditions and chemical reagents. *Dermatology.* 2006;212 Suppl 1(Suppl 1):119-123.
15. Ma B, Linden YS, Gundy PM, Gerba CP, Sobsey MD, Linden KG. Inactivation of coronaviruses and phage Phi6 from irradiation across UVC wavelengths. *Environ Sci Technol Lett.* 2021;8:425-430.
16. Darnell MESK, Feinstone SM, Taylor DR. Inactivation of the coronavirus that induces severe acute respiratory syndrome, SARS-CoV. *J Virol Methods.* 2004;121:85-91.
17. Ruetalo N, Businger R, Schindler M. Rapid, dose-dependent and efficient inactivation of surface dried SARS-CoV-2 by 254 nm UV-C irradiation. *Euro Surveill.* 2021;26:2001718.
18. Boegel SJ, Gabriel M, Sasges M, et al. Robust evaluation of ultraviolet-C sensitivity for SARS-CoV-2 and surrogate coronaviruses. *Microbiol Spectr.* 2021;9:e0053721.
19. Storm N, McKay LGA, Downs SN, et al. Rapid and complete inactivation of SARS-CoV-2 by ultraviolet-C irradiation. *Sci Rep.* 2020;10:22421.
20. Inagaki H, Saito A, Sugiyama H, Okabayashi T, Fujimoto S. Rapid inactivation of SARS-CoV-2 with deep-UV LED irradiation. *Emerg Microbes Infect.* 2020;9:1744-1747.
21. Kitagawa H, Nomura T, Nazmul T, et al. Effectiveness of 222-nm ultraviolet light on disinfecting SARS-CoV-2 surface contamination. *Am J Infect Control.* 2021;49:299-301.
22. Heilingloh CS, Aufderhorst UW, Schipper L, et al. Susceptibility of SARS-CoV-2 to UV irradiation. *Am J Infect Control.* 2020;48:1273-1275.
23. Patterson EI, Prince T, Anderson ER, et al. Methods of inactivation of SARS-CoV-2 for downstream biological assays. *J Infect Dis.* 2020;222:1462-1467.
24. Sabino CP, Sellera FP, Sales-Medina DF, et al. UV-C (254 nm) lethal doses for SARS-CoV-2. *Photodiagnosis Photodyn Ther.* 2020;32:101995.
25. Eickmann M, Gravemann U, Handke W, et al. Inactivation of three emerging viruses – severe acute respiratory syndrome coronavirus, Crimean-Congo haemorrhagic fever virus and Nipah virus – in platelet concentrates by ultraviolet C light and in plasma by methylene blue plus visible light. *Vox Sang.* 2020;115:146-151.
26. Biasin M, Bianco A, Pareschi G, et al. UV-C irradiation is highly effective in inactivating SARS-CoV-2 replication. *Sci Rep.* 2021;11:6260.
27. Ma B, Gundy PM, Gerba CP, Sobsey MD, Linden KG. UV inactivation of SARS-CoV-2 across the UVC spectrum: KrCl* excimer, mercury-vapor, and light-emitting-diode (LED) sources. *Appl Environ Microbiol.* 2021;87:e0153221.
28. Walker CM, Ko G. Effect of ultraviolet germicidal irradiation on viral aerosols. *Environ Sci Technol.* 2007;41:5460-5465.
29. Buonanno M, Welch D, Shuryak I, Brenner DJ. Author correction: Far-UVC light (222 nm) efficiently and safely inactivates airborne human coronaviruses. *Sci Rep.* 2021;11:19569.
30. Qiao Y, Yang M, Marabella IA, et al. Greater than 3-log reduction in viable coronavirus aerosol concentration in ducted ultraviolet-C (UV-C) systems. *Environ Sci Technol.* 2021;55:4174-4182.
31. Nicolo MS, Rizzo MG, Palermo N, Gugliandolo C, Cuzzocrea S, Guglielmino SPP. Evaluation of Betacoronavirus OC43 and SARS-CoV-2 elimination by Zefero air sanitizer device in a novel laboratory recirculation system. *Pathogens.* 2022;11:221.
32. Xie X, Muruato A, Lokugamage KG, et al. An infectious cDNA clone of SARS-CoV-2. *Cell Host Microbe.* 2020;27:841-848.
33. Ruetalo N, Businger R, Althaus K, et al. Antibody response against SARS-CoV-2 and seasonal coronaviruses in nonhospitalized COVID-19 patients. *mSphere.* 2021;6:e01145-20.
34. Cutler TD, Zimmerman JJ. Ultraviolet irradiation and the mechanisms underlying its inactivation of infectious agents. *Anim Health Res Rev.* 2011;12:15-23.

35. Blazquez E, Rodriguez C, Rodenas J, et al. Evaluation of the effectiveness of the SurePure turbulator ultraviolet-C irradiation equipment on inactivation of different enveloped and non-enveloped viruses inoculated in commercially collected liquid animal plasma. *PLoS One*. 2019;14:e0212332.

36. Oh C, Sun PP, Araud E, Nguyen TH. Mechanism and efficacy of virus inactivation by a microplasma UV lamp generating monochromatic UV irradiation at 222 nm. *Water Res*. 2020;186:116386.

37. Inagaki H, Saito A, Kaneko C, Sugiyama H, Okabayashi T, Fujimoto S. Rapid inactivation of SARS-CoV-2 variants by continuous and intermittent irradiation with a deep-ultraviolet light-emitting diode (DUV-LED) device. *Pathogens*. 2021;10:754.

SUPPORTING INFORMATION

Additional supporting information can be found online in the Supporting Information section at the end of this article.